

## RESEARCH ARTICLE

# A Formula for Successful Transmission Probability in Opportunistic Networks Under Memory-Time Correlated Channel Availability

**SHARHABEEL H. ALNABELSI**<sup>1,2</sup>, (Member, IEEE),  
**AND HAYTHEM A. BANY SALAMEH**<sup>1,3</sup>, (Senior Member, IEEE)

<sup>1</sup>College of Engineering, Al Ain University, Al Ain, United Arab Emirates

<sup>2</sup>Computer Engineering Department, Faculty of Engineering Technology, Al-Balqa Applied University, Al-Salt 19117, Jordan

<sup>3</sup>Telecommunications Engineering Department, Yarmouk University, Irbid 21163, Jordan

Corresponding author: Sharhabeel H. Alnabelsi (alnabsh1@bau.edu.jo)

This work was supported in part by the ASPIRE Award for Research Excellence (AARE-2020), Abu Dhabi, United Arab Emirates, under Grant AARE20-161.

**ABSTRACT** Dynamic Spectrum Access (DSA) technology in wireless Cognitive Radio Networks (CRNs) provides opportunistic access for unlicensed users, also known as Secondary Users (SUs), which can offer huge bandwidth to enable future wireless communication. Mainly, this technology aims to improve the end-to-end throughput by allowing SUs to exploit the licensed channels only when their licensed users, also known as Primary Users (PUs), are not using them. Most existing communication protocols designed for CRNs are based on the assumption that the channel availability time is considered based on a memoryless distribution for PUs arrivals. Unfortunately, this assumption is impractical because the PU channels' activity and availability are memory-time correlated. Worse yet, designing communication protocols for CRNs under this assumption can result in overestimating the Probability of Success (PoS) for SU packet transmissions, resulting in severe degradation in network performance in realistic scenarios. This paper derives a closed-form formula under memory-time correlation for channel availability that quantifies the PoS for SUs' packet transmission in CRNs. This will empower the network designers to get practical expectations about network efficiency rather than the overestimated PoS. Therefore, this work is also useful for emerging wireless networks with multi-hop routing, such as 5G, 6G, vehicular networks, etc., which incorporate DSA techniques. Our numerical and simulation results demonstrate that the PoS is overestimated in most of the literature due to adopting memoryless-based distribution in modeling channels' availability; such overestimation can impact communication protocol decisions, resulting in severe network performance degradation.

**INDEX TERMS** Primary users, secondary users, the Internet of Things, probability of success, memory-based distribution.

## I. INTRODUCTION

Dynamic Access Networks, also known as Cognitive Radio Networks (CRNs), have recently received huge attention due to their capability to efficiently utilize the available spectrum bands in the future generations of large-scale wireless networks such as Internet of Things (IoTs), 5G, and 6G. In these networks, users are deployed on a large scale. Thus, a huge spectrum of resources is needed. The Cognitive Radio (CR)

technology is proposed as a solution to this problem, in which the unused spectrum bands of the licensed users, known as Primary Users (PUs), are opportunistically exploited by the unlicensed users, known as Secondary Users (SUs), which results in increased network throughput [1], [2], [3], [4]. CRNs are based on the so-called Dynamic Spectrum Access (DSA) techniques, in which the SUs must switch between the available channels when their associated PUs becomes active. In other words, if the PU of the currently used channel by the SU becomes active again, the SU must vacate this channel immediately and switch to another available

The associate editor coordinating the review of this manuscript and approving it for publication was Cesar Vargas-Rosales<sup>1</sup>.

channel [5], [6]. CRNs have unique operation requirements, including spectrum sensing, channel assignment protocols, routing mechanisms, and routing protection [7], [8], [9], [10], [11], [12].

Different spectrum sensing techniques were developed in CRNs [13], [14], accurate sensing is a major factor that ensures the proper channels selection for SUs, hence, more stable multi-hop routing. Moreover, the accurate sensing decision reduces the number of channels switching for SUs along the transmission hops, thereby, the end-to-end transmission time is reduced, i.e., throughput is increased. Moreover, CRNs require should be aware about jamming by malicious attackers that interrupt SUs transmission, hence the end-to-end throughput is negatively affected. Thus, different protection protocols were developed to protect the SUs transmission [15], [16]. On the other hand, sometimes the channels are heterogeneous in terms of capacity, interference, harmful environmental noise, etc. Thus, a special attention is needed to assign channels efficiently to SUs such that the end-to-end throughput is [17], [18].

The nature of wireless communication networks is, in general, characterized as multi-hop multi-channel networks. In Cognitive Radio-IoTs (CR-IoTs), the selection of a route and its associated channels is crucial for the network performance [19], [20]. The proper route and channel selection results in reducing the end-to-end packet transmission delay. In fact, route selection and channel assignment is a very challenging task in multi-hop CRNs [21], [22], [23]. In such networks, the route and channel assignment should be performed such that the end-to-end Probability of Success (PoS) for SUs' packet transmission is maximized.

Most existing communication protocols designed for CRNs are based on the assumption that PU arrival (i.e., busy and idle channel states) are memoryless or have no time correlation. While this assumption cannot satisfy the realistic scenarios in which channel availability is memory-time correlated. Worse yet, wrong routing and channel assignment decisions can negatively impact the overall network throughput, especially under highly correlated PUs activities across time. Therefore, there is a need to consider the end-to-end time correlation for the channels' availability in deriving the PoS and selecting the operating routes and channels. The derived PoS metric should be used for designing channel assignment and routing protocols for CR-IoT networks. In other words, when a route is selected based on channel availability along its communication hops, these availability statuses may change during the routing time. Thus, the PoS under the memoryless assumption is overestimated. Therefore, in this work, we are motivated to derive a closed-form formula based on the memory-time property of channel availability. Our derived formula captures the memory-time property of channel correlation. Thus, the actual PoS of SU packet transmission can be found.

In this work, we evaluate our derived PoS formula through simulation. The derived expression reveals that PoS is overestimated when the traditional formula is used because it

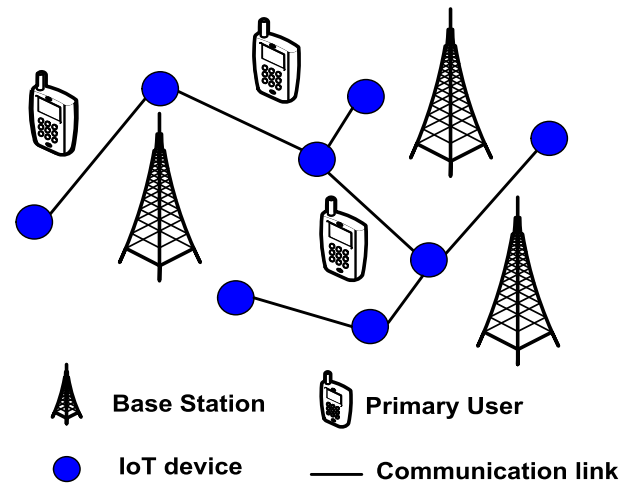


FIGURE 1. Network model.

assumes a memoryless-time correlation of channel availability. In this work, our main contributions are summarized as follows:

- Deriving a closed-form formula based on the memory-time property of channel availability to capture the time-correlation for channels' availability process.
- Capturing the actual PoS for packet transmission by utilizing our developed closed-form formula.
- Evaluating our derived PoS closed-form formula through simulations under multi-hop routing scenarios.
- Demonstrating that using the traditional formula that assumes a memoryless-time correlation of channel availability overestimates the PoS for packet transmission.

The remainder of this paper is organized as follows: Section II discusses the related work, and the system model is introduced in Section III. The derivation of the closed-form formula for the PoS of packet transmission under the memory-correlation assumption, using the derived formula in multi-hop multi-channel routing in CRNs, and an illustrative example are discussed in Section IV. Section V presents the performance evaluation, including numerical evaluation in addition to simulation results. Finally, the conclusions are summarized in Section VI.

## II. RELATED WORK

A probabilistic approach for selecting an idle channel is proposed in [24] that requires the channel's state information. In their work, the problem of keeping re-sensing the same channel while searching for the newly available channels is resolved in the proposed approach. Moreover, the authors developed a concurrent sensing and spectrum prediction platform to enhance the SUs throughput. A cooperative spectrum sensing model based on the Rayleigh fading channel and the non-fading AWGN channel is proposed in [25]. This model evaluates the probability of success for idle spectrum detection. Also, a medium access control protocol based on time slotting is proposed for cooperative spectrum sensing in

CR ad-hoc networks [26]. In this model, the probability of success for SUs and PUs is found based on the PU's coverage radius, transmission distance, and the number of SUs in the area.

Authors in [27] derived the cumulative distribution and probability density functions for the needed packet transmission time. Moreover, an adaptive SUs power transmission technique is developed. Also, in [28], an approximate expression is found for the probability of packet transmission error in the cooperative communication of CRNs, where the developed model is based on queuing theory. Moreover, an approximate expression for the probability of packet transmission error is derived in [29] for SUs communication, in addition to providing an evaluation for the overall throughput and delay. The proposed model operates under both fixed and adaptive power transmission.

Unfortunately, the PoS for packet transmission in all the aforementioned related work is evaluated based on the assumption of memoryless-time channel correlation. In other words, they assumed a memoryless arrival distribution for PUs, e.g., exponential distribution, which implies that the channel's availability time also follows a memoryless distribution. Unfortunately, this assumption is impractical because the channel's availability across time is correlated (i.e., memory-time correlation) [30], [31], [32]. Thus, our main motivation in this work is considering the memory-time channel correlation when assigning channels in multi-hop multi-channel routing. Therefore, a memory-based distribution is used in our analysis when we derive the closed-form formula for the PoS for packet transmission. The derived PoS formula is used for selecting the channel with the highest PoS when assigning channels in multi-hop routing in CRNs or dynamic access networks.

To the best of our knowledge, this is the first work for deriving a closed-form formula for the PoS of packet transmission in dynamic spectrum access networks. Our derived formula gives the actual PoS, which will help the network designers model and operate the network based on a realistic evaluation to meet the quality of service requirements effectively.

### III. SYSTEM MODEL

We consider an IoT-CRN environment consists of a group of PUs, IoT devices, and a set of channels. The IoT-CRN can coexist with different types of licensed networks, e.g., cellular networks, as depicted in Figure 1. In this network model, IoT devices represent the unlicensed users or the SUs that can co-exist with the licensed users or the PUs. The cellular network consists of base stations providing access to their PUs using their licensed channels. On the other hand, the IoT devices act as ad-hoc multi-hop wireless networks when establishing communications links (i.e., no central controller) based on the availability of licensed channels. The PUs' channel availability states are "ON" and "OFF" and are generally distributed; the "ON" state means the channel is currently busy, while the "OFF" state means the channel is currently not used by the PUs. We assume the IoT devices

use suitable sensing strategies that mainly depend on the cooperative sensing techniques and the usage of a common control channel for control packet exchange [1], [2], [3], [4].

The IoT-CRN requires a multi-hop route when delivering packets; thus, when a route is established between a source and a destination IoT device, all candidate routes should be explored, and the one with the highest throughput (i.e., the highest PoS for packet transmission) is selected. It is assumed that a channel assignment strategy that selects the channels over hops that gives the highest PoS is adopted. Therefore, a PoS metric should be adopted to assess the overall PoS for each candidate route and select the route with the highest overall PoS.

The used PoS metric or formula for packet transmission must be based on a memory-time correlated model to capture the actual remaining time for a given channel. For example, assume the actual available time for a given channel is 50 ms. Let this channel availability starts at time  $t$ ; however, it is used by the SU at a later time,  $t + \Delta t$ , say  $\Delta t = 20$  ms. The remaining idle/residual time is  $50 - 20 = 30$  ms. Thus, the residual available time is only 30 ms, not 50 ms. Hence, the required packet transmission time using this channel must be less or equal to 30 ms in order to have a successful transmission. This fact can be reflected by considering a memory-based distribution for the time of the channel's availability.

### IV. THE PoS ANALYSIS

At each hop along the selected route, the SUs select the channel that produces the highest data rate/capacity. Channel's capacity depends on its bandwidth, transmission power, environmental noise, etc. Due to the special nature of CRNs as it is based on DSA techniques, where the available transmission time of a channel, say channel  $i$ , is based on its average service/available/idle time, denoted as  $\mu_i$ , (idle time means when the PU is not transmitting over this channel, which is actually the available time for the SU for transmitting). Thus, the PoS for packet transmission by SUs depends on the available time in addition to the needed packet's transmission time. In general, the PoS for packet transmission over channel  $i$  is defined as follows;

$$PoS^{(i)} = P_r[tx^{(i)} \leq T_{idle}^{(i)}], \quad (1)$$

where  $PoS^{(i)}$ ,  $tx^{(i)}$ , and  $T_{idle}^{(i)}$  denote the PoS for packet transmission, needed transmission time, and available/idle time over channel  $i$ , respectively. While  $tx^{(i)} = \frac{D}{R^{(i)}}$ , where  $R^{(i)}$  denote the data rate of channel  $i$  and  $D$  denote the packet size.

Consequently, a higher service time and/or data rate increases the PoS. In other words, selecting one of the available channels over a given link depends on the transmission time and the channel's average service time. Therefore, it is possible to select a channel with a lower data rate rather than a channel with a higher data rate because its average idle time is greater. When the average idle time is higher, the PoS for transmitting one instance of a packet without interruption by the PU activity increases.

### A. PoS FORMULA UNDER MEMORY-TIME CORRELATED CHANNEL AVAILABILITY

The formula used, in most of the existing literature, for evaluating the PoS for a SU's packet transmission, over an idle channel  $i$ , is based on a memoryless-based distribution, where it is assumed that the PUs arrivals have a memoryless-time correlation. Specifically, for channel  $i$ , the idle duration was assumed to be an exponentially distributed random variable with an average idle duration of  $\mu_i$ . Based on this assumption and by substituting the CDF of the exponential distribution of the idle time [33] (i.e.,  $F_{T_{idle}^{(i)}}(t_x^{(i)}) = 1 - e^{-\frac{t_x^{(i)}}{\mu_i}}$ , where  $\mu_i$  denote channel  $i$  average idle time that can be measured empirically [34], [35]), the  $PoS_{memless}^{(i)}$  can be derived as:

$$\begin{aligned} PoS_{memless}^{(i)} &= P_r[T_{idle}^{(i)} \geq t_x^{(i)}] \\ &= 1 - F_{T_{idle}^{(i)}}(t_x^{(i)}) \\ &= 1 - (1 - e^{-\frac{t_x^{(i)}}{\mu_i}}) \\ &= e^{-\frac{t_x^{(i)}}{\mu_i}}. \end{aligned} \quad (2)$$

**Definition 1 (Channel's residual time):** It is defined as the remaining time from the available/idle time at this channel before its corresponding PU becomes active (the residual time is less than or equal to the idle time).

The remaining channel's time is based on its availability, i.e., the residual available time is memory correlated [30], [31], [32]. Consequently, we derive the PoS for packet transmission based on the memory-time correlation of the channel's availability, in which the recent activity of this channel is captured. A more accurate assessment is produced, reflecting the practical activity over this channel compared to memoryless-based PoS evaluation. Thus, a better decision can be made when selecting the operating channels.

The author in [36] proposed a general-form equation that finds a formula for the CDF of residual time (this time can be used for packet transmission), denoted by  $F_r(t_x^{(i)})$ , based on the CDF of the idle time, denoted by  $F_{T_{idle}}(t)$  are given, as follows;

$$F_r(t_x^{(i)}) = \frac{\int_0^{t_x^{(i)}} (1 - F_{T_{idle}}(t)) dt}{\mu_i} \quad (3)$$

In general, the packet is transmitted successfully over a given channel, say channel  $i$ , if and only if its transmission time,  $t_x^{(i)}$ , is less than or equal to the remaining channel's idle time (the residual time), denoted by  $T_r^{(i)}$ . Hence, the PoS for SU's packet transmission over channel  $i$  can be expressed as follows;

$$PoS^{(i)} = P(T_r^{(i)} \geq t_x^{(i)}) = 1 - F_r(t_x^{(i)}). \quad (4)$$

To proceed with our analysis for the PoS and without loss of generality, we assume that the channels' availability time for each PU channel follows a memory-based distribution, specifically, the chi-squared distribution [30], [37], [38] (unlike the exponential distribution, which has the

memoryless property). The memory property allows capturing the channel's availability distribution over the routing period/timeline in multi-hop routing in CRNs.

To find the PoS for SU's packet transmission under a chi-squared distribution, denoted by  $PoS_{mem}$ , we first find the CDF of the idle time distribution that depends on the memory-based chi-squared distribution, denoted by  $F_{T_{idle}^{mem}}^{(i)}(t_x^{(i)})$ . Let  $f(t, k)$  denote the chi-squared distribution's probability density function (PDF), where  $t$  is a positive real number, and  $k$  is a positive integer number that denotes the degree of freedom. In our proposed model,  $t$  and  $k$  variables are mapped to  $t_x^{(i)}$  and  $\mu_i$ , respectively. Hence, the  $F_{T_{idle}^{mem}}^{(i)}(t_x^{(i)})$  for channel  $i$  is found as follows;

$$F_{T_{idle}^{mem}}^{(i)}(t_x^{(i)}) = \frac{\gamma(\frac{\mu_i}{2}, \frac{t_x^{(i)}}{2})}{\Gamma(\frac{\mu_i}{2})} \quad (5)$$

where  $\gamma$  denote the lower incomplete-gamma function and  $\Gamma$  denote the gamma function.

The term  $\gamma(\frac{\mu_i}{2}, \frac{t_x^{(i)}}{2})$  was defined in [39] and [40] as follows;

$$\gamma(\frac{\mu_i}{2}, \frac{t_x^{(i)}}{2}) = \int_0^{\frac{t_x^{(i)}}{2}} t^{\frac{\mu_i}{2}-1} e^{-t} dt \quad (6)$$

By using the table of integrals [41], the integral in (6) is equivalent to the following expression;

$$\Gamma(\frac{\mu_i}{2}) - \gamma(\frac{\mu_i}{2}, \frac{t_x^{(i)}}{2}) \quad (7)$$

In addition, it was shown that the term  $\Gamma(\frac{\mu_i}{2})$  in (5) can be rewritten as follows [42];

$$= (\frac{\mu_i}{2} - 1)! \quad (8)$$

Finally, by substituting the expressions found in (7) and (8) into (5),  $F_{T_{idle}^{mem}}^{(i)}(t_x^{(i)})$  can be expressed as:

$$F_{T_{idle}^{mem}}^{(i)}(t_x^{(i)}) = \frac{\Gamma(\frac{\mu_i}{2}) - \gamma(\frac{\mu_i}{2}, \frac{t_x^{(i)}}{2})}{(\frac{\mu_i}{2} - 1)!} \quad (9)$$

Second, we find the CDF of the residual time under memory-based channel availability distribution (chi-squared distribution), denoted by  $F_r(t_x^{(i)})_{mem}$ , by substituting the obtained CDF of  $F_{T_{idle}^{mem}}^{(i)}(t_x^{(i)})$  found in (9) into (3) and evaluate its associated integration, a closed-form expression for the memory-based CDF for  $F_r(t_x^{(i)})_{mem}$  is obtained as in (10), shown at the bottom of the next page. Finally, to find the PoS for packet transmission at channel  $i$ ,  $PoS_{mem}^{(i)}$ , substitute the  $F_r(t_x^{(i)})_{mem}$  expression that is found in (10) into (4). Hence, it becomes as follows;

$$PoS_{mem}^{(i)} = 1 - F_r(t_x^{(i)})_{mem}. \quad (11)$$

### B. PoS AND ROUTING IN CRNS

The main issue in performing efficient routing in multi-channel multi-hops CRNs is how to find the route along with its associated channel assignment such that the end-to-end

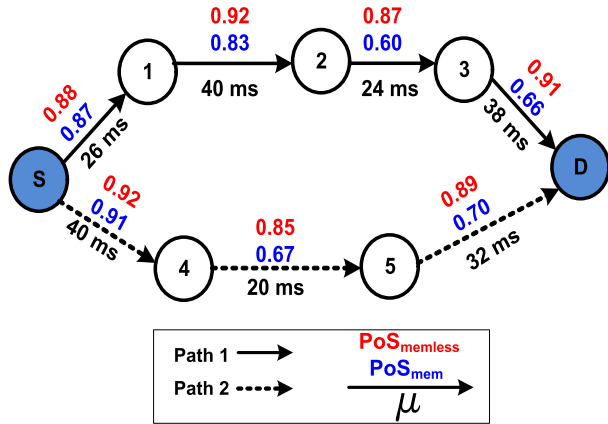


FIGURE 2. An illustrative example scenario.

PoS is maximized. We assume that the dynamic decode-and-forward mechanism is used for routing packets where the packet is forwarded to the next hop only when it is successfully decoded, as this allows to avoid the error propagation effect in multi-hop routing [43], [44]. This mechanism has been previously used in [33], [45], and [46] for multi-hop routing. Let us introduce some notations and routing metrics before discussing our illustrative example (in the next subsection) that demonstrates the effectiveness of our derived PoS expression in capturing the actual success probability for packet transmission, as follows;

- $\mathcal{H}_p$  denote the set of hops along path  $p$ .
- $\mathcal{C}_{H(p,h)}$  denote the set of available channels at path  $p$  over hop  $h$ .
- $H(p, h)$  denote hop  $h$  over path  $p$ .
- $c(p, h, i)$  denote the  $i$ th element in the set of available channels at hop  $h$  over path  $p$ .
- $PoS_{memless}^{c(p,h,i)}$  denote the PoS for channel  $i$  at hop  $h$  along path  $p$  for memoryless-based channel assignment.
- $PoS_{mem}^{c(p,h,i)}$  denote the PoS for channel  $i$  at hop  $h$  along path  $p$  for memory-based channel assignment.
- $PoS_{memless}^{H(p,h)}$  denote the PoS for memoryless-based channel assignment at path  $p$  over hop  $h$ .
- $PoS_{mem}^{H(p,h)}$  denote the PoS for memory-based channel assignment at path  $p$  over hop  $h$ .
- $PoS_{memless}^p$  denote the PoS for path  $p$  when the memoryless-based channel assignment is used.
- $PoS_{mem}^p$  denote the PoS for path  $p$  when the memory-based channel assignment is used.

In general, the  $PoS_{memless}^{H(p,h)}$  was found by selecting the channel from the set of available channels over hop  $h$  along path  $p$ ,  $\mathcal{C}_{H(p,h)}$ , which gives the highest PoS [47], using (2),

as follows;

$$PoS_{memless}^{H(p,h)} = \max \left\{ PoS_{memless}^{c(p,h,1)}, PoS_{memless}^{c(p,h,2)}, \dots, PoS_{memless}^{c(p,h,i)}, \dots, PoS_{memless}^{c(p,h,|\mathcal{C}_{H(p,h)}|)} \right\}. \quad (12)$$

where  $c(p, h, i)$  denote the  $i$ th element in the set of available channels at path  $p$  over hop  $h$  ( $\mathcal{C}_{H(p,h)}$ ).

The PoS of a given path, say path  $p$ , when the memoryless-based channel assignment is used can be found as follows;

$$PoS_{memless}^p = \min \left\{ PoS_{memless}^{H(p,1)}, PoS_{memless}^{H(p,2)}, \dots, PoS_{memless}^{H(p,i)}, \dots, PoS_{memless}^{H(p,|\mathcal{H}_p|)} \right\}. \quad (13)$$

where  $H(p, i)$  denote the  $i$ th hop over path  $p$ .

The  $PoS_{mem}^{H(p,h)}$  is found by selecting the channel from the set of ( $\mathcal{C}_{H(p,h)}$ ), that gives the highest PoS, using (11), as follows;

$$PoS_{mem}^{H(p,h)} = \max \left\{ PoS_{mem}^{c(p,h,1)}, PoS_{mem}^{c(p,h,2)}, \dots, PoS_{mem}^{c(p,h,i)}, \dots, PoS_{mem}^{c(p,h,|\mathcal{C}_{H(p,h)}|)} \right\}. \quad (14)$$

where  $c(p, h, i)$  denote the  $i$ th element in the set of ( $\mathcal{C}_{H(p,h)}$ ).

The PoS of a given path, say path  $p$ , when memory-based channel assignment is used can be found as follows;

$$PoS_{mem}^p = \min \left\{ PoS_{mem}^{H(p,1)}, PoS_{mem}^{H(p,2)}, \dots, PoS_{mem}^{H(p,i)}, \dots, PoS_{mem}^{H(p,|\mathcal{H}_p|)} \right\}. \quad (15)$$

where  $H(p, i)$  denote the  $i$ th hop over path  $p$ .

### C. ILLUSTRATIVE EXAMPLE

The impact of using the overestimated PoS metric (memoryless-based distribution) can result in selecting a less efficient route. To demonstrate this negative effect, Figure 2 shows an example for two candidate paths from a Source SU (S) to a Destination SU (D); this example clearly demonstrates our motivation in this work. The PoS for packet transmission at each link over its channel, say channel  $i$ , is evaluated based on memoryless-based channel assignment,  $PoS_{memless}^{(i)}$ , and it is also evaluated based on memory-based channel assignment,  $PoS_{mem}^{(i)}$ , by using (2) and our derived closed-form equation, in (11), respectively. For the sake of demonstration simplicity, in Figure 2, we assume each hop has only one available channel, say channel  $i$ . Hence, (12)

$$F_r(t_x^{(i)})_{mem} = \frac{1}{\mu_i(\frac{\mu_i}{2} - 1)!} \int_0^{t_x^{(i)}} \left( \left( \frac{\mu_i}{2} - 1 \right)! - \Gamma\left(\frac{\mu_i}{2}\right) + \gamma\left(\frac{\mu_i}{2}, \frac{t}{2}\right) \right) dt$$

$$= t_x^{(i)} \left( \frac{\mu_i}{2} - 1 \right)! - t_x^{(i)} \gamma\left(\frac{\mu_i}{2}\right) + 2 \left( \gamma\left(\frac{\mu_i}{2} + 1\right) + \frac{-2^{-\mu_i/2} e^{-t_x^{(i)}/2} t_x^{(i)\frac{\mu_i}{2}+1} + (t_x^{(i)} - \mu_i) \Gamma\left(\frac{\mu_i}{2} + 1, \frac{t_x^{(i)}}{2}\right)}{\mu_i} \right). \quad (10)$$

is considered over one channel when the memoryless-based channel assignment is used, and also (14) is considered over one channel when the memory-based channel assignment is used. In both cases, the PoS for these channels is evaluated and labeled at each hop, as shown in Figure 2.

To find the PoS for path 1 and path 2 under the memoryless-based channel assignment, (13) is used. Thus,  $PoS_{memless}^1 = \min\{0.88, 0.92, 0.87, 0.91\} = 0.87$ , and  $PoS_{memless}^2 = \min\{0.92, 0.85, 0.89\} = 0.85$ . Consequently, Path 1 has a higher PoS than path 2; hence, it will be selected for routing when the memoryless-based channel assignment strategy is adopted. On the other hand, to find the actual PoS for path 1 and path 2 under the memory-based channel assignment, (15) is used. Thus,  $PoS_{mem}^1 = \min\{0.87, 0.83, 0.60, 0.66\} = 0.60$ , and  $PoS_{mem}^2 = \min\{0.91, 0.67, 0.70\} = 0.67$ . Consequently, Path 2 has a higher PoS than Path 1, and hence, it will be selected for routing when the memory-based channel assignment is adopted. In conclusion, the actual PoS for path 1 is overestimated when adopting the memoryless-based channel assignment strategy. However, when the memory-based channel assignment strategy is adopted, the actual PoS is captured for both paths, where path 2 has a higher actual PoS. Therefore, path 2 should be selected for routing to enhance system performance.

## V. PERFORMANCE EVALUATION

In this section, we investigate the impact of different network parameters in order to evaluate our developed closed-form formula. MATLAB 2021a is used to find the numerical and simulation results for the studied probabilistic formulas.

### A. NUMERICAL EVALUATION

We first demonstrate the impact of the memory-based arrival nature of PU transmissions by comparing the PoS metric under memory-based PU arrival (the derived formula based on the chi-squared distribution) with that of the unrealistic existing memoryless-based formula (based on the exponential distribution) for 200 realizations for a given PU's channel, say channel  $i$ , with an average idle time of  $\mu_i$  and bandwidth of 10 Mbps. Figure 3 illustrates that the baseline formula overestimates the PoS for packet transmission compared to our derived memory-based PoS formula for different average idle times. In this figure, when  $\mu_i$  is very low (2 ms), both formulas give the same PoS. When  $\mu_i$  is moderate (8 ms and 12 ms), the overestimation for the memoryless-based formula increases compared to the memory-based formula. On the other hand, when  $\mu_i$  is high (18 ms), the overestimation for the memoryless-based formula becomes less. That is due to the fact that when  $\mu_i$  is high, the needed transmission time becomes less or equal to the channel's available time with a higher probability.

Now, we evaluate the PoS of the packet transmission for memoryless-based (i.e., exponential distribution - as in (2)) and memory-based (chi-square distribution - as in (11)) channel assignment for one-hop transmission. In this analysis, for evaluation purposes, we assume there is one channel

over the studied transmission hop-link. Every instance of the numerical results is the average of 2000 iterations. In every iteration, the transmission power is re-evaluated based on the randomly selected distance between the IoT-SU transmitter and the IoT-SU receiver; this distance range is [10 - 140] m. The channel's rate,  $R$ , is evaluated based on the Shannon-Hartley's theorem that is subject to the Additive white Gaussian Noise (AWGN),  $R = B \log_2(1 + SNR)$ , where  $B$  denotes the channel's bandwidth, and  $SNR$  denote the signal to noise ratio. The used carrier frequency is 900 MHz, the packet size is 2 KB, and the path-loss exponent is 4. We also set the average idle time for the considered channel, say channel  $i$ , to  $\mu_i$ .

Let us evaluate the performance of the memoryless-based formula (based on the exponential distribution) and the memory-based formula (based on the chi-squared distribution) regarding the PoS for channel assignment. Figure 4 illustrates the PoS versus the average idle time,  $\mu$ , and for different channels' bandwidth. In Figures 4(a), 4(b), and 4(c), the channel's bandwidth is 5 Mbps, 10 Mbps, and 15 Mbps, respectively. The average idle time is between 2 ms and 50 ms, where the transmission power's mean is set to 1 watt. In Figure 4(a), as the average idle time,  $\mu$ , increases, the difference in performance between the two formulas decreases. In general, results of Figure 4 show that the difference in performance between the two formulas decreases as bandwidth increases. For example, when comparing the difference in performance found in Figure 4(a) to the one found in Figure 4(c), the difference becomes less. That is because when the bandwidth increases, the required packet transmission time decreases, consequently increasing the PoS.

In Figure 5, we study the PoS versus the SUs transmission power for different channels' average idle times. In Figures 5(a), 5(b), and 5(c), the channel's average idle time,  $\mu$ , is set to 8 ms, 12 ms, and 18 ms, respectively, and the bandwidth is set to 10 Mbps. In Figure 5(a), when the average idle time is 8 ms, the memoryless-based channel assignment method overestimates the PoS compared to the actual PoS found based on the memory-based channel assignment method. Recall that, in this subsection, we study the PoS for one channel for a given transmission. Moreover, when the average idle time increases,  $\mu = 18$  ms, as in Figure 5(c), the PoS overestimation ratio decreases. Moreover, increasing the SUs transmission power has less significance on the PoS than increasing the channel's average idle time.

## B. SIMULATION EVALUATION

### 1) SIMULATION SETUP

The data rate for each SU is taken from the range  $[R_{min} - R_{max}]$ , and this range is varied as [0.2Mbps-5Mbps], and also the results are re-evaluated when the data rate is between [10Mbps-30Mbps]. In every simulation run, the data rate for each channel, at each hop-link over the studied route, is randomly chosen between  $[R_{min} - R_{max}]$ . The data rates are randomly selected to capture the independent fading effect

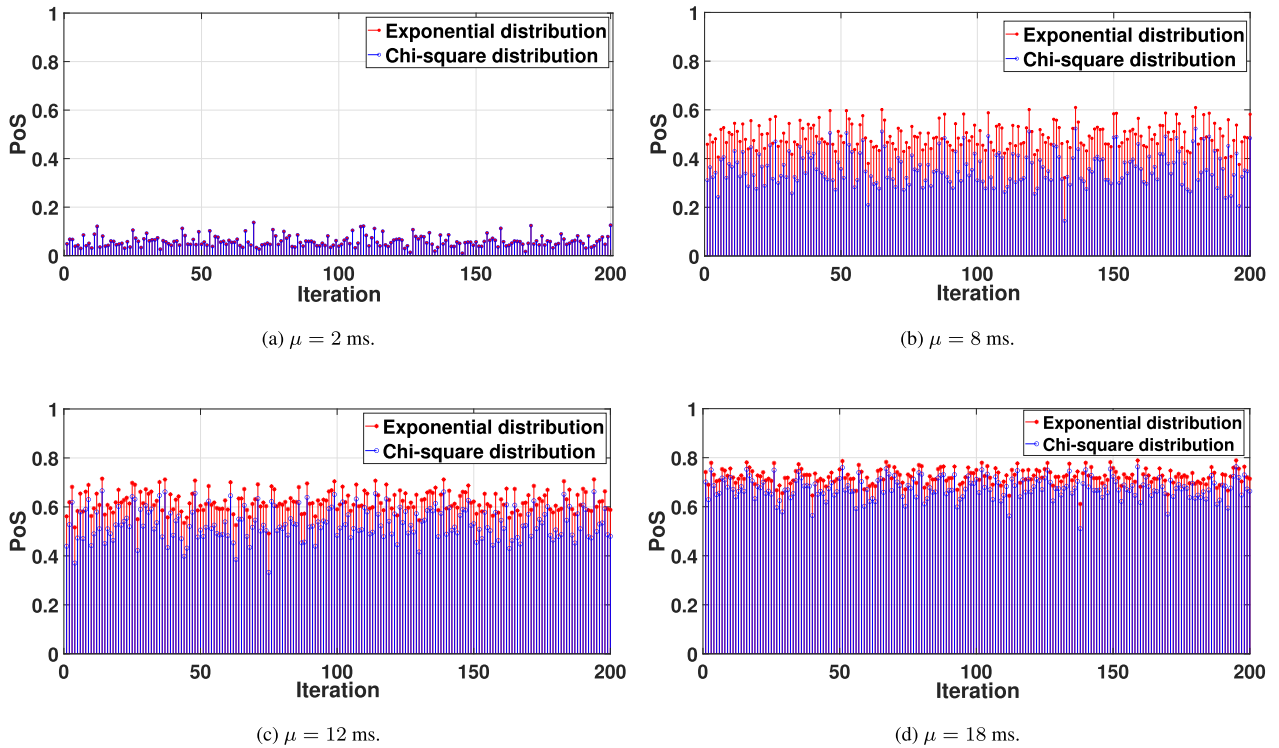


FIGURE 3. PoS evaluation for exponential and chi-squared distributions formulas for different channels' average idle time ( $\mu$ ), BW = 10 Mbps.

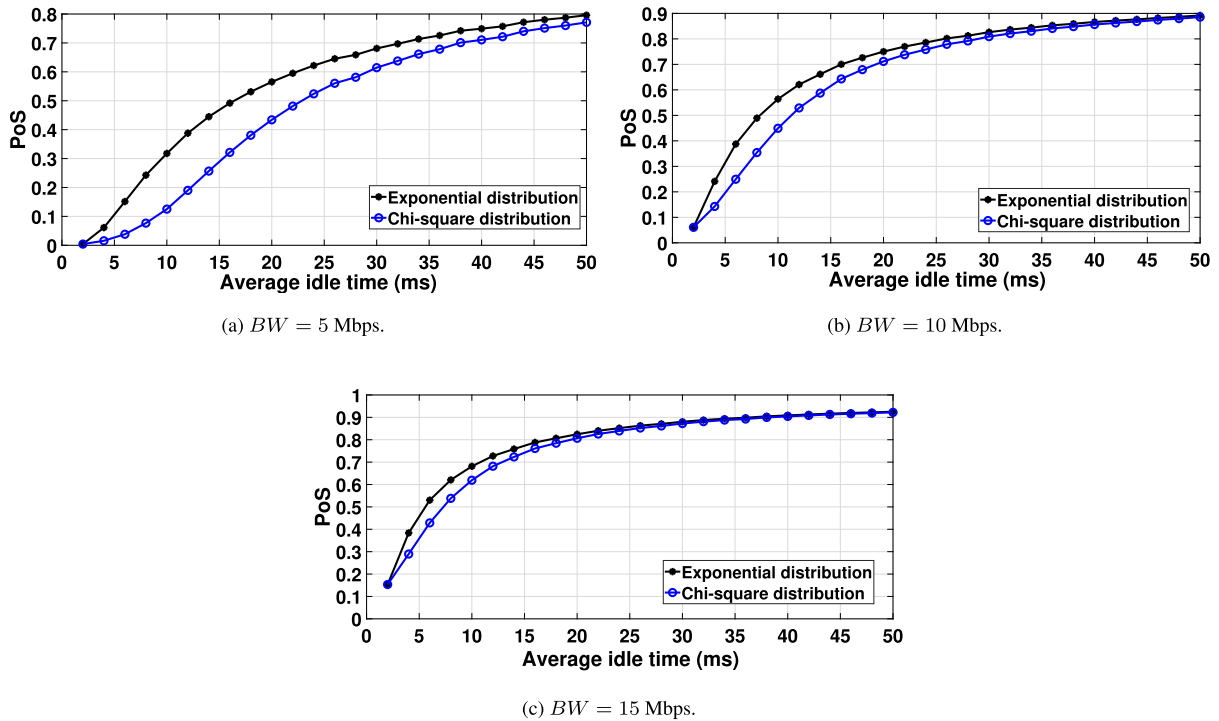


FIGURE 4. PoS evaluation of exponential and chi-squared distributions formulas with respect to channel's average idle time ( $\mu$ ).

over the different channels [48]. Moreover, at each simulation run, the SUs are redeployed such that the minimum distance between any pair of SUs is 5 m. The probability of a channel being available or busy is re-assessed in every simulation run based on its distribution. Every instance of the simulation

results is the average of 2000 iterations. In the simulation study, there are 12 PUs' channels. Their average idle/service time ( $\mu_i$ ) is  $\zeta \times \{6, 2, 4, 8, 10, 6, 2, 4, 2, 10, 2, 8\}$  ms, where  $\zeta$  denote the PUs' arrival severity factor (i.e., higher arrival severity means the average channel's idle/service time,  $\mu_i$ ,

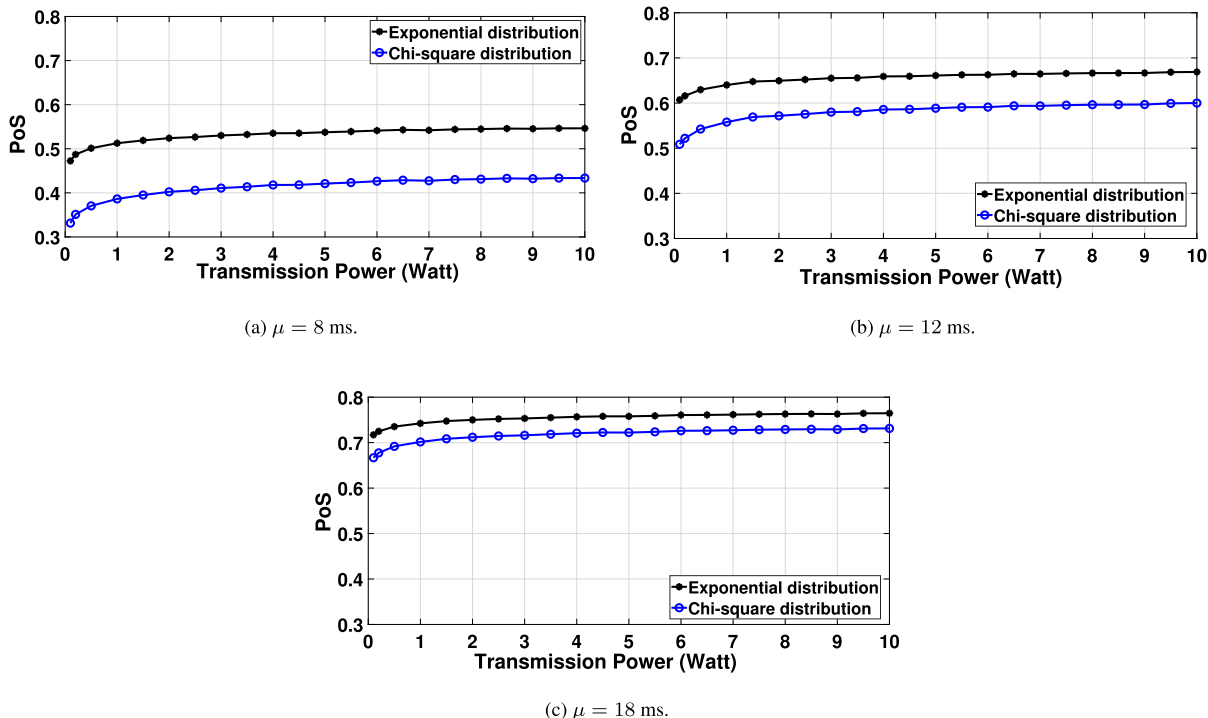


FIGURE 5. PoS evaluation of exponential and chi-squared distributions formulas with respect to the SUs transmission power (Watt).

becomes less). We evaluate the PoS for Low Arrival (LA), Medium Arrival (MA), and High Arrival (HA) when  $\zeta$  is 0.8, 0.4, and 0.1, respectively.

In every iteration, a set of  $K$ -shortest paths are found [49]. For every investigated path, say path  $p$ , out of the found  $\mathcal{K}$  paths, the PoS based on memoryless channel assignment,  $PoS_{memless}^p$ , is found using (13). The path with the highest PoS is selected. After that, the actual PoS of the selected path, say path  $\bar{p}$ ,  $PoS_{mem}^{\bar{p}}$ , is found using (15).

2) SIMULATION RESULTS

In this subsection, we study the effect of channels’ availability, the number of channels on the evaluated PoS for SU’s transmission, and the effect of low and high data rates. Results have revealed that memoryless-based channel assignments overestimated the PoS. At the same time, the memory-based one gives the actual PoS for packet transmission in multi-hop multi-channel routing in CRNs.

a: IMPACT OF CHANNELS AVAILABILITY

The effect for the probability of channels being idle,  $P_{idle}$ , on the PoS for the transmitted packet is studied for multi-hop routing. The value of  $P_{idle}$  is varied between 0.2 and 0.9 in order to assess the effect of low, medium, and high channels’ availability on the PoS for the memoryless-based and memory-based channel assignment methods. Figure 6 shows the PoS versus  $P_{idle}$  for different PUs arrival severity and when the number of channels is 6. The memoryless-based channel assignment method overestimates the PoS compared to the memory-based method. In Figures 6(a), 6(b), and 6(c)

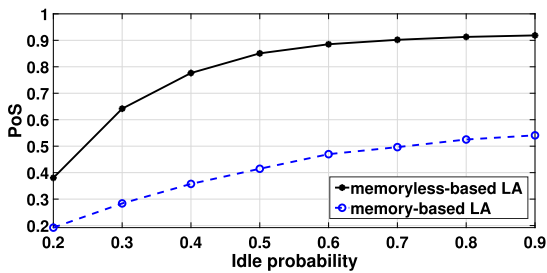
results are evaluated when the arrival rate is low, medium, and high, respectively. The PoS increases as the idle probability increases. Also, the PoS increases when the PU’s arrival severity decreases. Figure 7 shows the PoS versus  $P_{idle}$  for different PUs arrival severity and when the number of channels is 12. The memoryless-based channel assignment method overestimates the PoS compared to the memory-based method, in Figures 7(a), 7(b), and 7(c) results are evaluated when the arrival rate is low, medium, and high, respectively. The PoS increases as the idle probability increase. Also, the PoS increases when the arrival severity decreases. Noting that the memoryless-based method overestimates the PoS regardless of the probability of channels being idle or the PU’s arrival severity.

For evaluation purposes, we have increased the data rate to be selected randomly between 10 Mbps and 30 Mbps while the other simulation parameters are not changed. Thus, the results in Figure 6 and Figure 7 are re-generated when the data rate is [10 Mbps - 30 Mbps] as shown in Figure 8 and Figure 9, respectively. The results show that the PoS for memory-based and memoryless-based channel assignment become very close to each other for low and medium PUs arrival rates; that is because when the data rate increases, the packet transmission time decreases. Thus, the PoS of packet transmission during the available or the remaining idle time increases since the packets need less time to be transmitted. On the other hand, when the PUs arrival rate is high, the memory-based channel assignment still outperforms the memoryless-based one for a different number of channels and different idle probabilities.

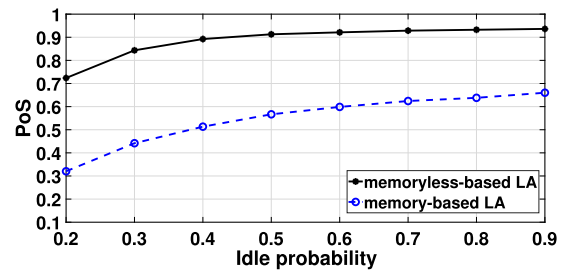


TABLE 1. PoS summary with low and high data rates.

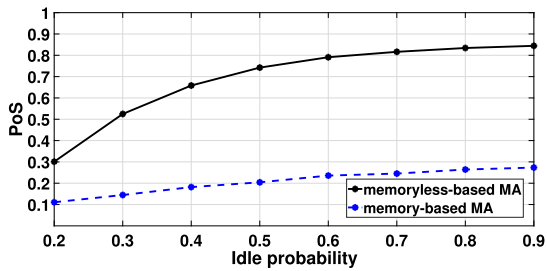
		PoS											
		Low Data Rate [0.2 Mbps - 5.0 Mbps]					High Data Rate [10 Mbps - 30 Mbps]						
		moderate $\mu_i$			High $\mu_i$		moderate $\mu_i$			High $\mu_i$			
$P_{idle}$		$PoS_{memless}$	$PoS_{mem}$	OE%	$PoS_{memless}$	$PoS_{mem}$	OE%	$PoS_{memless}$	$PoS_{mem}$	OE%	$PoS_{memless}$	$PoS_{mem}$	OE%
0.5		0.82	0.30	173%	0.90	0.58	55%	0.97	0.85	14%	0.98	0.92	6%
0.9		0.88	0.39	125%	0.93	0.65	43%	0.98	0.89	10%	0.98	0.95	3%



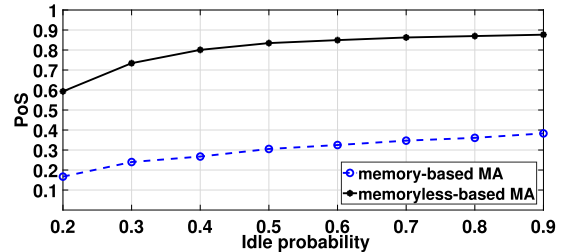
(a) Low arrival severity,  $\zeta = 0.8$ .



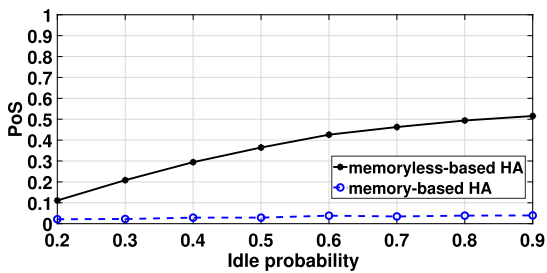
(a) Low arrival severity,  $\zeta = 0.8$ .



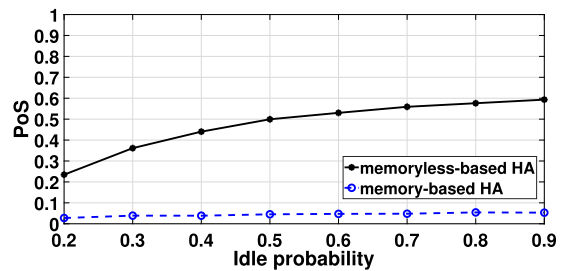
(b) Medium arrival severity,  $\zeta = 0.4$ .



(b) Medium arrival severity,  $\zeta = 0.4$ .



(c) High arrival severity,  $\zeta = 0.1$ .



(c) High arrival severity,  $\zeta = 0.1$ .

FIGURE 6. PoS performance with respect to  $P_{idle}$  for 6 PU channels, and data rate of [0.2 Mbps - 5.0 Mbps].

The summary table, Table 1, compares the memory-based and the memoryless-based processes for modeling the

FIGURE 7. PoS performance with respect to  $P_{idle}$  for 12 PU channels, and data rate of [0.2 Mbps - 5.0 Mbps].

channel availability, in which a summary of the PoS for low and high data rates are presented with moderate and

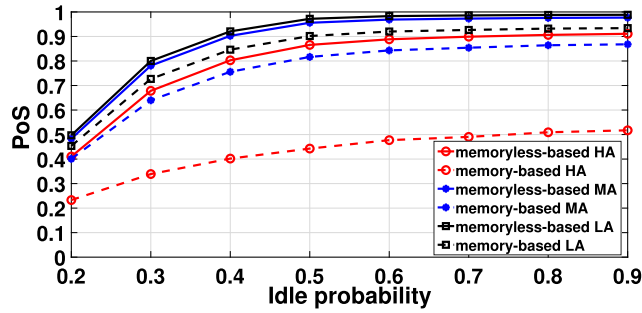


FIGURE 8. PoS performance with respect to  $P_{idle}$  for 6 PU channels, and data rate of [10 Mbps - 30 Mbps].

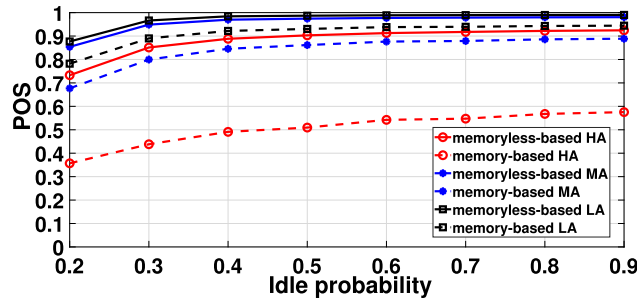
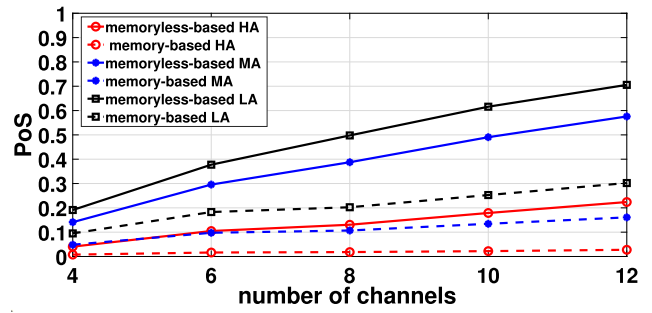


FIGURE 9. PoS performance with respect to  $P_{idle}$  for 12 PU channels, and data rate of [10 Mbps - 30 Mbps].

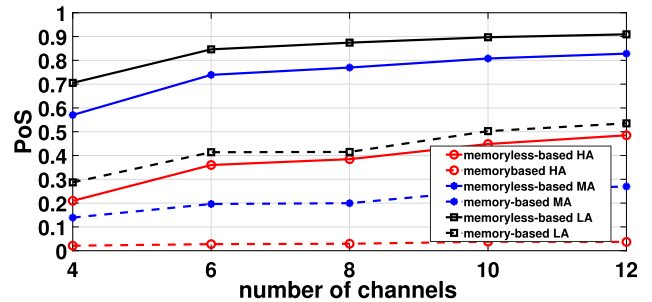
high average idle times, namely moderate  $\mu_i$  and high  $\mu_i$  respectively. Moreover, we have evaluated the Overestimation Error percentage ( $OE\%$ ) for all cases as illustrated in the given table. In this table, the low data rate values are extracted from Figures 7(a) and 7(b), which are considered as high  $\mu_i$  and moderate  $\mu_i$ , respectively. While the corresponding values of the high data rate are extracted from Figure 9, specifically the values for low arrival (LA) and moderate arrival (MA) that are considered as high  $\mu_i$  and moderate  $\mu_i$ , respectively. Clearly, when the data rate is low, the  $OE\%$  values are high (especially when  $\mu_i$  is moderate) compared to the ones when the data rate is high. As a result, when the data rate is low, assuming memory-based processes gives more realistic values for modeling channel availability in multi-hop routing. However, when the data rate is high assuming memory-based processes yields a result that is not significantly different from assuming memoryless-based processes.

#### b: IMPACT OF THE AVAILABLE PU CHANNELS

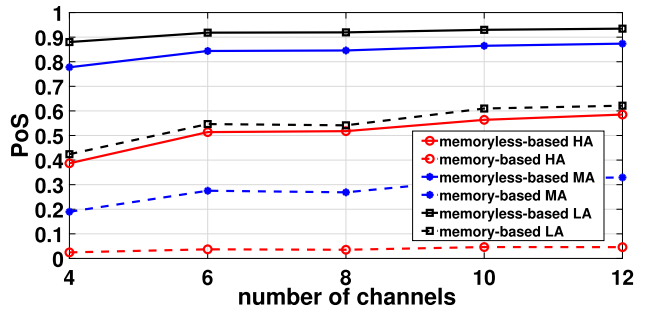
The effect of the number of channels on the PoS for packet transmission is studied. Figure 10 shows the PoS versus the number of channels. Specifically, Figure 10(a), Figure 10(b), and Figure 10(c) show the PoS when the probabilities of channels being idle are 0.2, 0.5, and 0.9, respectively. The results reveal that when our proposed formula, based on memory-time correlation, is used in routing decisions, the overall



(a)  $P_{idle} = 0.2$ .



(b)  $P_{idle} = 0.5$ .

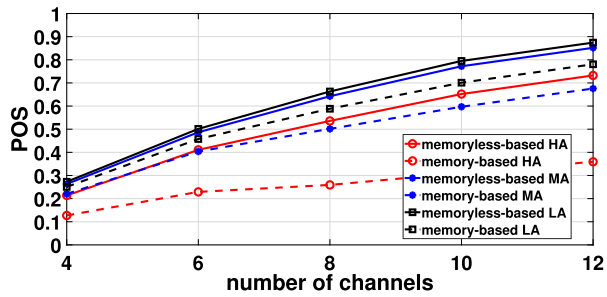


(c)  $P_{idle} = 0.9$ .

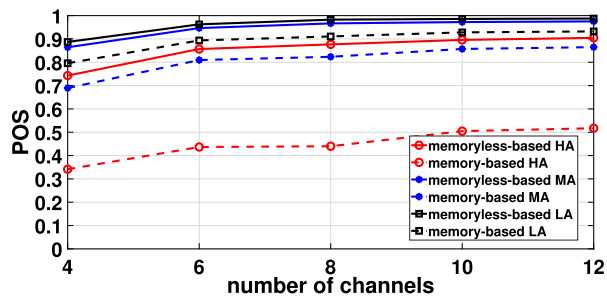
FIGURE 10. PoS performance with respect to the number of channels when the data rate is [0.2 Mbps - 5.0 Mbps].

PoS for routing is higher than using the memoryless-based formula for a different number of channels and different idle probabilities.

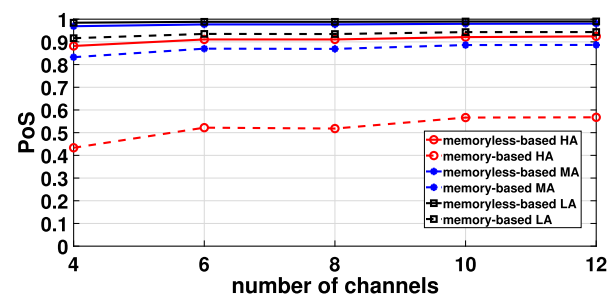
For evaluation purposes, we increase the data rate to be selected randomly between 10 Mbps and 30 Mbps. The other simulation parameters are not changed. The results of Figure 10 are regenerated when the data rate is [10 Mbps - 30 Mbps] as shown in Figure 11. The results show that the PoS for memory-based and memoryless-based channel assignments become very close to each other for low and medium PUs arrival rates (as explained earlier). However, when the arrival rate is high, the memory-based channel assignment still outperforms the memoryless-based one for a different number of channels and different idle probabilities.



(a)  $P_{idle} = 0.2$ .



(b)  $P_{idle} = 0.5$ .



(c)  $P_{idle} = 0.9$ .

**FIGURE 11.** PoS performance with respect to the number of channels when the data rate is [10 Mbps - 30 Mbps].

## VI. CONCLUSION

The paper derived a closed-form formula for evaluating the Probability of Success (PoS) for SU's packet transmissions in IoT-CRN, which considers memory-time correlation in PU channel availability. This formula improves upon existing PoS formulas in the literature, which assume memoryless-time correlation and tend to overestimate the PoS for SUs. The proposed formula is useful in designing communication protocols for multi-hop multi-channel IoT-CRN and can help identify routes with the highest actual PoS. The formula was assessed through extensive numerical and simulation evaluations, demonstrating its practicality over the existing memory-less time-correlated PoS formula under various network parameters. The PoS is accurately estimated using the proposed formula, the number of needed re-transmissions decreases, reducing the overall transmission power, enhancing the achieved end-to-end throughput, and prolonging the network lifetime for IoT devices. As future work, we plan

to utilize our developed closed-form formula to study the performance of channel assignment for half-duplex and full-duplex transmission techniques in multi-hop routing, and to design an energy-efficient multi-hop routing protocol that is based on modeling channels' activity as a memory-based process that captures the actual PoS for packets' transmission. In addition, we plan to empirically validate the performance of our routing protocol using a realistic test-bed platform.

## REFERENCES

- [1] Y. Arjoune and N. Kaabouch, "A comprehensive survey on spectrum sensing in cognitive radio networks: Recent advances, new challenges, and future research directions," *Sensors*, vol. 19, no. 1, p. 126, Jan. 2019.
- [2] O. M. Al-Kofahi, H. M. Almasaeid, and H. Al-Mefleh, "Efficient on-demand spectrum sensing in sensor-aided cognitive radio networks," *Comput. Commun.*, vol. 156, pp. 11–24, Apr. 2020.
- [3] M. Liu, H. Zhang, Z. Liu, and N. Zhao, "Attacking spectrum sensing with adversarial deep learning in cognitive radio-enabled Internet of Things," *IEEE Trans. Rel.*, pp. 1–14, 2022.
- [4] M. Miazi, "An energy-efficient common control channel selection mechanism for cognitive radio ad-hoc networks," *Ann. Telecommun.-Annales des Télécommunications*, vol. 70, no. 1, pp. 11–28, 2015.
- [5] F. Hu, B. Chen, and K. Zhu, "Full spectrum sharing in cognitive radio networks toward 5G: A survey," *IEEE Access*, vol. 6, pp. 15754–15776, 2018.
- [6] V. Nallarasana and K. Kottilingam, "Spectrum management analysis for cognitive radio iot," in *Proc. Int. Conf. Comput. Commun. Informat. (ICCCI)*, Jan. 2021, pp. 1–5.
- [7] A. Dhawan and C. K. Jha, "Routing and security issues in cognitive radio ad hoc networks (CRAHNS)—A comprehensive survey," in *Proc. Int. Conf. Innov. Comput. Commun.* Singapore: Springer, 2020, pp. 489–501.
- [8] A. M. Almasoud and A. E. Kamal, "Robust provisioning of multicast sessions in cognitive radio networks," in *Proc. Int. Wireless Commun. Mobile Comput. Conf. (IWCMC)*, Aug. 2014, pp. 417–422.
- [9] Q. Medhat Salih, Md. A. Rahman, F. Al-Turjman, and Z. R. M. Azmi, "Smart routing management framework exploiting dynamic data resources of cross-layer design and machine learning approaches for mobile cognitive radio networks: A survey," *IEEE Access*, vol. 8, pp. 67835–67867, 2020.
- [10] S. Sivakumar, T. Chellatamilan, and R. Sathiyaseelan, "Discovery of optimal multicast routes in MANETs using cross-layer approach and fuzzy logic support system," *Cluster Comput.*, vol. 22, no. S5, pp. 11467–11476, Sep. 2019.
- [11] A. J. Kadhim and S. A. H. Seno, "Energy-efficient multicast routing protocol based on SDN and fog computing for vehicular networks," *Ad Hoc Netw.*, vol. 84, pp. 68–81, Mar. 2019.
- [12] E. Ezenogho, "Effect of an incumbent user on unlicensed users channels in cognitive radio networks: An overlay performance evaluation," *J. Commun.*, vol. 13, no. 6, pp. 275–283, 2018.
- [13] K. Kockaya and I. Develi, "Spectrum sensing in cognitive radio networks: Threshold optimization and analysis," *EURASIP J. Wireless Commun. Netw.*, vol. 2020, no. 1, pp. 1–19, Dec. 2020.
- [14] M. S. Gupta and K. Kumar, "Progression on spectrum sensing for cognitive radio networks: A survey, classification, challenges and future research issues," *J. Netw. Comput. Appl.*, vol. 143, pp. 47–76, Oct. 2019.
- [15] V. Nallarasana and K. Kottursamy, "Cognitive radio jamming attack detection using an autoencoder for CRiot network," *Wireless Pers. Commun.*, vol. 127, pp. 1–17, Aug. 2021.
- [16] R. Derbas, "Routing algorithm for multi-hop iot cognitive radio networks under proactive jamming attacks," M.S. thesis, Arabic Digit. Library, Yarmouk Univ., 2020.
- [17] E. Ezenogho and V. M. Srivastava, "Performance analysis of heterogeneous channel assembling strategies in cognitive radio networks," *Int. J. Eng. Technol. Innov.*, vol. 7, no. 2, pp. 98–116, 2017.
- [18] E. Ezenogho and V. M. Srivastava, "Channel assembling strategy in cognitive radio networks: A queuing based approach," *Int. J. Commun. Antennas Propag.*, vol. 7, no. 1, pp. 31–47, 2017.
- [19] D. Tarek, A. Benslimane, M. Darwish, and A. M. Kotb, "Survey on spectrum sharing/allocation for cognitive radio networks Internet of Things," *Egyptian Informat. J.*, vol. 21, no. 4, pp. 231–239, Dec. 2020.

- [20] E. Esenogho, K. Djouani, and A. M. Kurien, "Integrating artificial intelligence Internet of Things and 5G for next-generation smartgrid: A survey of trends challenges and prospect," *IEEE Access*, vol. 10, pp. 4794–4831, 2022.
- [21] F. Aghaei and A. Avokh, "MRCSC: A cross-layer algorithm for joint multicast routing, channel selection, scheduling, and call admission control in multi-cell multi-channel multi-radio cognitive radio wireless networks," *Pervas. Mobile Comput.*, vol. 64, Apr. 2020, Art. no. 101150.
- [22] M. Devi, N. Sarma, and S. K. Deka, "A double auction framework for multi-channel multi-winner heterogeneous spectrum allocation in cognitive radio networks," *IEEE Access*, vol. 9, pp. 72239–72258, 2021.
- [23] R. Ahmed, Y. Chen, B. Hassan, and L. Du, "CR-iotNet: Machine learning based joint spectrum sensing and allocation for cognitive radio enabled iot cellular networks," *Ad Hoc Netw.*, vol. 112, Mar. 2021, Art. no. 102390.
- [24] P. Thakur, A. Kumar, S. Pandit, G. Singh, and S. N. Satashia, "Performance analysis of cognitive radio networks using channel-prediction-probabilities and improved frame structure," *Digit. Commun. Netw.*, vol. 4, no. 4, pp. 287–295, Nov. 2018.
- [25] C. Sudhamani, S. Ram, and A. Saxena, "Estimation of success probability in cognitive radio networks," in *Proc. Int. Conf. Commun. Cyber Phys. Eng.*, in Lecture Notes in Electrical Engineering, vol. 500, 2019, pp. 279–285.
- [26] J. Gao, "On the successful transmission probability of cooperative cognitive radio ad hoc networks," *Ad Hoc Netw.*, vol. 58, pp. 99–104, Apr. 2017.
- [27] L. Sibomana, H.-J. Zepernick, H. Tran, and C. Kabiri, "Packet transmission time for cognitive radio networks considering interference from primary user," in *Proc. 9th Int. Wireless Commun. Mobile Comput. Conf. (IWCMC)*, Jul. 2013, pp. 791–796.
- [28] I. Dimitriou and T. Phung-Duc, "Analysis of cognitive radio networks with cooperative communication," in *Proc. 13th EAI Int. Conf. Perform. Eval. Methodologies Tools*, May 2020, pp. 192–195.
- [29] N. Ben Halima and H. Boujemaa, "Approximate expressions of packet error probability, throughput and delay for cognitive radio networks using fixed and adaptive transmit power," *Telecommun. Syst.*, vol. 71, no. 1, pp. 19–30, May 2019.
- [30] J. Lunden, V. Koivunen, A. Huttunen, and H. V. Poor, "Spectrum sensing in cognitive radios based on multiple cyclic frequencies," in *Proc. 2nd Int. Conf. Cognit. Radio Oriented Wireless Netw. Commun.*, Aug. 2007, pp. 37–43.
- [31] C. Lu, W. Xu, H. Shen, J. Zhu, and K. Wang, "MIMO channel information feedback using deep recurrent network," *IEEE Commun. Lett.*, vol. 23, no. 1, pp. 188–191, Jan. 2019.
- [32] L. Yu, Y. Guo, Q. Wang, C. Luo, M. Li, W. Liao, and P. Li, "Spectrum availability prediction for cognitive radio communications: A DCG approach," *IEEE Trans. Cognit. Commun. Netw.*, vol. 6, no. 2, pp. 476–485, Jun. 2020.
- [33] H. Tran-Dang and D. Kim, "Link-delay and spectrum-availability aware routing in cognitive sensor networks," *IET Commun.*, vol. 14, no. 20, pp. 3639–3651, Dec. 2020.
- [34] L. Fang, X. Cheng, H. Wang, and L. Yang, "Idle time window prediction in cellular networks with deep spatiotemporal modeling," *IEEE J. Sel. Areas Commun.*, vol. 37, no. 6, pp. 1441–1454, Jun. 2019.
- [35] S. Odou, S. Martin, and K. Al Agha, "Idle channel time estimation in multi-hop wireless networks," in *Proc. IEEE Int. Conf. Commun.*, Jun. 2009, pp. 1–5.
- [36] S. Kamal and B. Nazar, "Performance evaluation of combining SMT-ETX metric with POS scheme for implementing multilayer multicast mobile ad hoc network (MANET) CRN," *IET Commun.*, vol. 14, no. 4, pp. 610–618, Mar. 2020.
- [37] I. B. Djordjevic, B. Vasic, M. Ivkovic, and I. Gabitov, "Achievable information rates for high-speed long-haul optical transmission," *J. Lightw. Technol.*, vol. 23, no. 11, pp. 3755–3763, Nov. 2005.
- [38] S. H. Kang and S.-M. Yoon, "Long memory properties in return and volatility: Evidence from the Korean stock market," *Phys. A, Stat. Mech. Appl.*, vol. 385, no. 2, pp. 591–600, Nov. 2007.
- [39] M. A. Chaudhry and S. M. Zubair, *On a Class of Incomplete Gamma Functions With Applications*. Boca Raton, FL, USA: CRC Press, 2001.
- [40] B. Hassibi and T. L. Marzetta, "Multiple-antennas and isotropically random unitary inputs: The received signal density in closed form," *IEEE Trans. Inf. Theory*, vol. 48, no. 6, pp. 1473–1484, Jun. 2002.
- [41] I. S. Gradshteyn and I. M. Ryzhik, *Table of Integrals, Series, and Products*. New York, NY, USA: Academic, 2014.
- [42] R. Vidunas, "Expressions for values of the gamma function," *Kyushu J. Math.*, vol. 59, no. 2, pp. 267–283, 2005.
- [43] D. Zheng, Y. Yang, L. Wei, and B. Jiao, "Decode-and-forward short-packet relaying in the Internet of Things: Timely status updates," *IEEE Trans. Wireless Commun.*, vol. 20, no. 12, pp. 8423–8437, Dec. 2021.
- [44] T. M. Hoang, B. C. Nguyen, N. N. Thang, M. Tran, and P. T. Tran, "Performance and optimal analysis of time-switching energy harvesting protocol for MIMO full-duplex decode-and-forward wireless relay networks with various transmitter and receiver diversity techniques," *J. Franklin Inst.*, vol. 357, no. 17, pp. 13205–13230, Nov. 2020.
- [45] M. Abdollahi, F. Eshghi, M. Kelarestaghi, and M. Bag-Mohammadi, "Opportunistic routing metrics: A timely one-stop tutorial survey," *J. Netw. Comput. Appl.*, vol. 171, Dec. 2020, Art. no. 102802.
- [46] N. Zhang, J. Guan, and S. Yin, "MSP: A routing metric for cognitive radio networks," in *Proc. 12th Int. Conf. Qual., Rel., Secur. Robustness Heterogeneous Netw.* South Korea: Springer, 2016, pp. 149–159.
- [47] R. Naveen Raj, A. Nayak, and M. S. Kumar, "Spectrum-aware cross-layered routing protocol for cognitive radio ad hoc networks," *Comput. Commun.*, vol. 164, pp. 249–260, Dec. 2020.
- [48] T. Shu, S. Cui, and M. Krunz, "WLC05-3: Medium access control for multi-channel parallel transmission in cognitive radio networks," in *Proc. IEEE Globecom*, Nov. 2006, pp. 1–5.
- [49] A. Madkour, W. G. Aref, F. U. Rehman, M. A. Rahman, and S. Basalamah, "A survey of shortest-path algorithms," 2017, *arXiv:1705.02044*.



**SHARHABEEL H. ALNABELSI** (Member, IEEE)

received the M.Sc. degree in computer engineering from The University of Alabama in Huntsville, USA, in 2007, and the Ph.D. degree in computer engineering from Iowa State University, USA, in 2012. He has been an Associate Professor with the Computer Engineering Department, Al-Balqa Applied University, Al-Salt, Jordan, since 2012. Currently, he is on leave as an Associate Professor with the Computer Engineering Department, Al Ain University, United Arab Emirates. His research interests include cognitive radio networks, wireless sensors networks, and network resources optimization. He is a member of honorary societies, including Eta Kappa Nu and Phi Kappa Phi. Also, he is a reviewer of many international conferences and journals.



**HAYTHEM A. BANY SALAMEH** (Senior Member, IEEE)

received the Ph.D. degree in electrical and computer engineering from The University of Arizona, Tucson, AZ, USA, in 2009. In the Summer of 2008, he was a member of the Research and Development Long-Term Evolution Development Group, Qualcomm Inc., San Diego, CA, USA. In the Summer of 2015, he was a Visiting Research Professor with the Telecommunications Systems and Networks Laboratory, Aristotle University of Thessaloniki, Greece. He is currently a Professor of wireless networking engineering with Al Ain University, United Arab Emirates, and Yarmouk University (YU), Irbid, Jordan. He is also the Dean of scientific research and graduate studies with Al Ain University. He is also a Visiting Professor with the Faculty of Computing, Staffordshire University, U.K. Recently, he has been involved in projects related to securing the iot communications, cognitive radios/SDRs, distributed resource management in full-duplex wireless networks, drone networking with AI support, communication protocols, with an emphasis on spectrum access, cross-layer design, and channel/power assignment. His research interests include wireless communications technology, artificial intelligence (AI)-based networking, the Internet of Things (iot) networking, and security protocols for delay-sensitive iot applications, with an emphasis on resource allocation, adaptive control, and distributed protocol design. He was a recipient of the Jordan Science Research Support Foundation Prestigious Award for Distinguished Research in the ICT Sector, in 2015, the Best Researcher Award for Scientific Colleges in YU, from 2015 to 2016, and the Jordan Science Research Support Fund Award for Creativity and Technological Scientific Innovation, in 2017. He was the Organizing Chair of the Seventh and Eighth International Conferences on Social Networks Analysis, Management and Security (SNAMS), in 2020 and 2021, and a Steering Committee Member of the Seventh and Eighth International Conference on Internet of Things: Systems Management, Security (iotSMS), in 2020 and 2021.